Absolute total cross sections for the scattering of 2–18-eV electrons by cesium atoms

B. Jaduszliwer and Y. C. Chan
Electronics Technology Center, The Aerospace Corporation, P. O. Box 92957, Los Angeles, California 90009
(Received 29 July 1991)

Absolute total cross sections for the scattering of electrons by cesium atoms between 2 and 18 eV have been measured using the atomic-recoil technique in the scattering-out mode. Our results are somewhat lower than those of Visconti, Slevin, and Rubin [Phys. Rev. A **3**, 1310 (1971)] above 2 eV.

PACS number(s): 34.80.−i

I. INTRODUCTION

Alkali-metal atoms have been traditionally chosen by electron-atom scattering experimentalists and theorists as common testing grounds. Since the body of work on electron–alkali-metal-atom collisions has become very large, we will not attempt to give a complete bibliography. Alkali-metal atomic beams are relatively easy to produce and detect, making them the target of choice in some of the earliest crossed-beams scattering experiments [1–6]. Alkali-metal atoms, consisting of a tightly bound noble-gas-like core plus a single, loosely bound valence electron, make ideal targets for studies of the role of spin in electron-atom collisions [2,7–12]. They can also be easily excited at visible or near-infrared wavelengths, which makes them convenient targets to study electron collisions with excited state atoms [13–21]. Recently, alkali-metal vapors also became the subject of collision studies involving positrons [22]. Because of the large oscillator strength of the transition coupling the nS ground state of an alkali-metal atom with its nP first excited state, few-state close-coupling calculations [23–28] have been extraordinarily successful in describing low-energy electron scattering by the alkali metals. At higher energies, those calculations lose validity. A number of different approaches [29–31] have been attempted to treat electron-atom scattering in the intermediate-energy regime in which few-state close-coupling calculations become unsatisfactory, while techniques like the Born approximation or its many variants may not yet be accurate enough.

Most of the experimental and theoretical work on electron collisions with alkali-metal atoms has been performed using sodium or potassium as targets. Lately, there has been a surge of interest on electron-cesium collisions, mainly because cesium, having a fairly high atomic number, is more likely than the rest of the stable alkali metals to display the effects of spin-orbit or other relativistic couplings on the electron scattering amplitudes. We have started a program to investigate the role of spin in electron collisions with cesium atoms, using optical techniques for atomic spin state preparation and analysis.

As a first experiment, we have measured absolute total electron scattering cross sections on cesium atoms. For the lighter alkali metals, two-state close-coupling calculations [23,24] yield total cross sections which are in very good agreement with experiment, but the results of previous measurements by Visconti, Slevin, and Rubin [5] (VSR) for cesium are significantly lower than the two-state close-coupling calculations of Karule [24] below the first inelastic threshold; above it, they agree better with the close-coupling calculations of Karule and Peterkop [23]. The energy range we have explored, between 2 and 18 eV, partially overlaps those measurements, and it is embedded in the intermediate-energy regime, currently the subject of considerable theoretical interest.

II. EXPERIMENT

Our measurements were performed using the atomic-recoil technique in the scattering-out mode, first described by Rubin, Perel, and Bederson [32]. The apparatus is shown schematically in Fig. 1. The cesium beam source is a two-chamber effusive oven, with the cesium reservoir heated up to about 200 °C, and the outlet chamber 25 °C hotter. Half of the cesium atoms in the beam have negative magnetic moments; these are velocity selected and collimated by a hexapole magnet. The cesium dimer concentration in the oven reservoir chamber is about [33] 1.7×10^{-3}, and is lowered somewhat by the higher temperature at the outlet chamber. Inserting the hexapole magnet triples the cesium beam intensity at the detection end of the atomic beam apparatus; since only the cesium atoms are focused by the hexapole magnet,

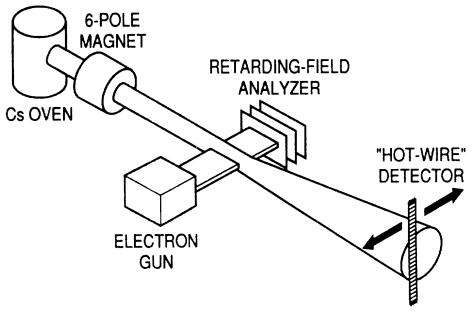

FIG. 1. Schematic view of the cesium atomic beam apparatus. The "hot-wire" detector can be displaced sideways to explore the angular distribution of atoms crossing the detector plane.

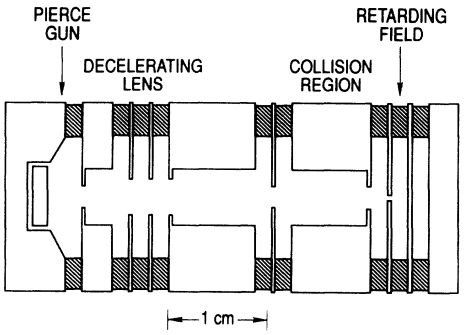

FIG. 2. Cross-sectional view of the electron gun. Dashed areas: alumina insulators. The electrodes are made of molybdenum. The Pierce gun employs an indirectly heated alkaline-earth oxide cathode.

and not the dimers, we conclude that the dimer fraction of the detected beam is well below 0.1%.

The atomic beam is cross fired by an orthogonal, ribbon-shaped electron beam; the experiment coordinate system is defined with the x axis pointing along the atomic beam and the z axis along the electron beam. The beams overlap region measures approximately 38, 2.3, and 1.6 mm along the x, y, and z axes, respectively; our technique does not require an accurate knowledge of the geometry of the overlap region. The electron gun, shown in cross section in Fig. 2, consists of a Pierce gun [34] with an indirectly heated alkaline-earth oxide cathode, a decelerating lens [35], an equipotential collision region where the electron and atomic beams intersect, and a retarding-field electron energy analyzer. The electron

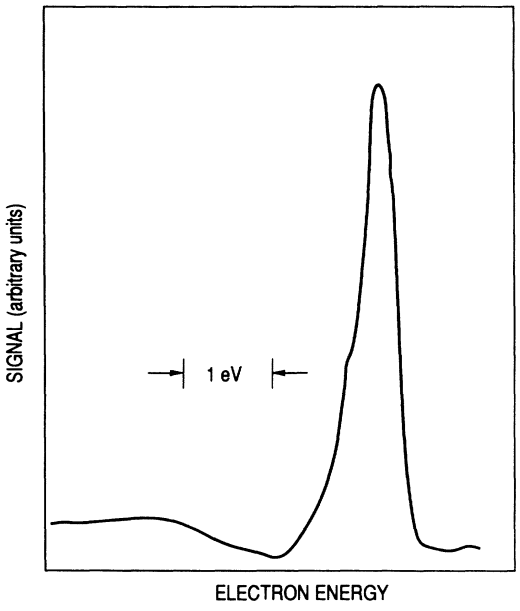

FIG. 3. Electron energy distribution, obtained from the measured transmission of the retarding field analyzer by differentiation. This distribution was measured at approximately 5-eV peak energy.

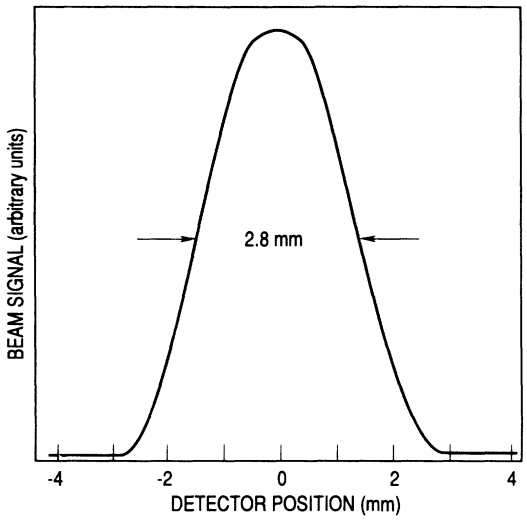

FIG. 4. Intensity profile of the cesium atomic beam at the detector plane.

beam can be prevented from entering the interaction region by applying a negative voltage at the center element of the decelerating lens. Figure 3 shows a typical electron energy distribution; the full width at half maximum (FWHM) of 400 meV is consistent with the cathode temperature.

The cesium atoms are detected at a distance $L = 914$ mm downstream from the collision volume by surface ionization on a hot tungsten wire. The resulting cesium ions are accelerated into the entrance slit of a 90° sector magnetic mass analyzer which discriminates against sodium or potassium ions diffusing off the hot tungsten wire. The ion current coming out through the mass analyzer slit is amplified by a high-current Channeltron electron multiplier. The cesium-atom detector can rotate in the

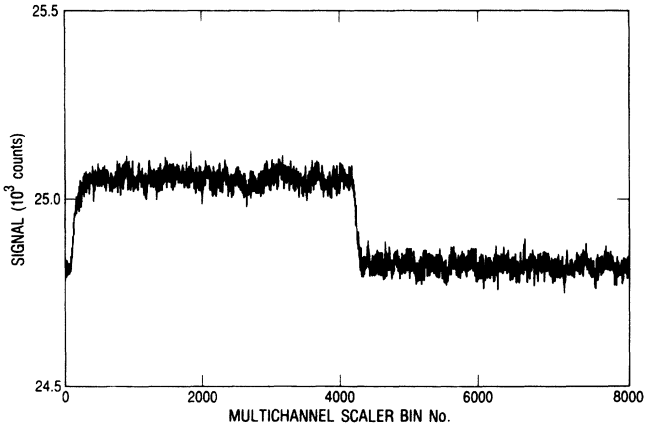

FIG. 5. Typical atomic beam signal collected in the MCS for a total cross-section measurement. Dwell time: ≈82 μs/bin, 8192 bins/scan, 2200 scans. The electron-gun current was turned off synchronously with the beginning of each scan, and turned on at middle on each scan. The electron energy in this case was 12 eV, and the electron current was 697 μA.

plane defined by the beams (the xz plane), about the center of the collision region. Figure 4 displays the intensity profile of the atomic beam, showing a 2.8-mm FWHM.

In the scattering-out recoil technique, the atomic beam intensity is monitored by the detector, positioned on the beam axis. If the electron beam is allowed to enter the interaction region (by switching the voltage at the center element of the decelerating lens from the negative cutoff voltage to the appropriate positive focusing voltage), some of the atoms in the beam will collide with electrons and will be recoiled away from the beam axis. The atomic beam current will be reduced by an amount [1] equal to the collision rate,

$$\Delta I_a = \sigma (I_e I_a / H) \langle 1/V \rangle \ , \tag{1}$$

where I_a and I_e are the atomic and electronic beam number currents, σ is the total electron-atom scattering cross section, H is the height of the atomic beam within the interaction region (3.79 mm, as defined by an entrance slit), and $\langle 1/V \rangle$ is the mean inverse atomic speed over the atomic beam speed distribution (which in this experiment is non-Maxwellian, determined mainly by the hexapole magnet). This assumes that the geometry of the beams overlap volume is such that all the collected electrons cross the atomic beam. As long as the detector is linear, $\Delta I_a / I_a = \Delta S_a / S_a$ (S_a being the detector signal), and so

$$\sigma = (\langle 1/V \rangle^{-1} H / I_e)(\Delta S_a / S_a) \ . \tag{2}$$

Thus, this technique allows us to determine absolute total cross sections without measuring the atomic beam density or calibrating the atomic detector (an absolute measurement of I_e is required).

Figure 5 shows typical beam signal data measured in a scattering-out experiment. The electron multiplier collector current is measured by an electrometer; the combined hot-wire plus electrometer time constant is about 5 ms. The analog output of the electrometer (approximately 1.7 V) is sampled by a voltage-to-frequency converter of our design (based on the Burr-Brown VFC320 IC chip), operating at 0.1 MHz/V; the output pulses are counted by and stored in a multichannel scaler (MCS) operated at 82 μs/bin with an 8-kbin scan. The MCS sweep and the beam on-off switching signal at the decelerating lens central electrode are triggered synchronously at about 1.5 Hz, and enough scans are accumulated to have the same resolution as a 15-bit analog-to-

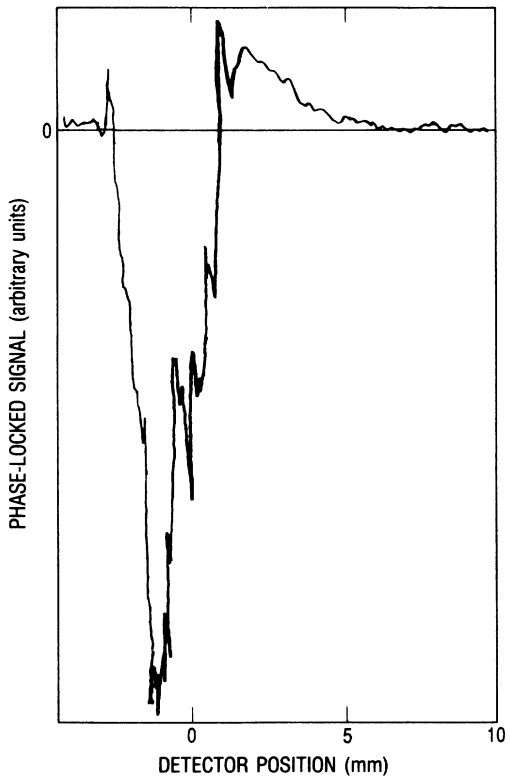

FIG. 6. 15-Hz component of the atomic detector signal vs detector position; the origin is set at the beam axis. The electron gun is chopped at 15 Hz, and the ac component of the atomic signal is detected synchronously. Atoms are predominantly recoiled away from the detector near the beam axis (scattering-out signal), and into the detector to the right of the beam axis (scattering-in signal). The prominent peak at $z \approx 2.3$ mm is the signature of forward electron scattering after impact excitation of the $6P$ atomic state. These data were obtained at 8.2-eV electron energy.

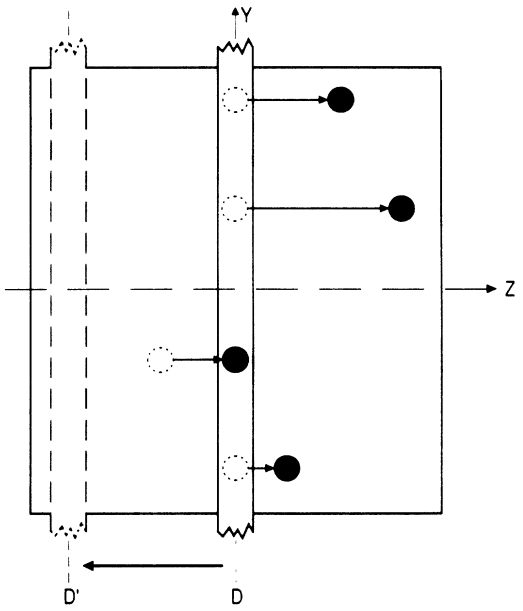

FIG. 7. Schematic mapping of the cesium atomic beam cross section at the detector plane. Atoms which, in the absence of collisions with electrons would cross the detector plane where indicated by open circles, will be deflected towards the right by collisional recoil and cross it where indicated by dark circles. Many of the atoms which would impact the detector at the center (D) will miss it (scattering out), while a few that would miss it will impact it (scattering in). Moving the detector towards the left (D') reduces the number of atoms available to be recoiled into the detector, thus reducing the scattering-in contribution to the signal.

digital converter (i.e., about 3×10^{-5}). The figure shows clearly how the atomic beam signal responds to the electron beam being switched off and on.

Equation (2) requires the determination of $\langle 1/V\rangle$; this is accomplished by using a technique discussed in more detail elsewhere [15]. Briefly, the electron beam is chopped at about 15 Hz and the phase-locked ac component of the atomic beam signal is measured while the atomic beam detector is displaced along the z axis. Results typical of such a measurement, when performed at electron energies higher than the cesium $6S$-$6P$ excitation threshold $eE^*\approx1.46$ eV, are shown in Fig. 6. The large negative signal near beam axis indicates that atoms are being recoiled predominantly away from the detector; as the detector moves away from the atomic beam, atoms begin to be recoiled predominantly into the detector, and the signal becomes positive. The pronounced peak in the scattering-in signal is the signature of forward electron scattering after impact excitation of the $6P$ state, and its positron, relative to the beam axis, is given by [15]

$$\Delta z_0=[(2me)^{1/2}L/M]\langle 1/V\rangle[E^{1/2}-(E-E^*)^{1/2}]\ , \quad (3)$$

where m,e are the electron mass and charge, M is the mass of the cesium atom, and eE is the electron energy. Thus, a measurement of Δz_0 determines $\langle 1/V\rangle$. In this experiment, $\langle 1/V\rangle^{-1}\approx(271\pm13)$ m/s, and it remained constant from day to day.

Equation (1) implicitly requires the atomic beam and detector to have negligible widths, since it assumes that collisions within the overlap volume will recoil atoms away from the detector, but not into it. As soon as the widths of the beam and detector become finite, a certain fraction of the collisions will recoil into the detector some atoms which otherwise would not be detected, as illustrated in Fig. 7. There will be two contributions of opposite signs to ΔS_a,

$$\Delta S_a=\Delta S_a(\text{out})-\Delta S_a(\text{in})\ , \quad (4)$$

but σ is related only to the scattering-out contribution, $\Delta S_a(\text{out})$. In general, the scattering-in contribution $\Delta S_a(\text{in})$ will depend on the shape of the small-angle differential cross section, atomic beam density distribution, atomic and electron momentum distributions, and detector geometry; Jaduszliwer *et al.* [36] analyzed $\Delta S_a(\text{in})$ in detail for the case of electron scattering by highly polar molecules, where the largely forward character of the differential cross section made it an important contribution to ΔS_a. The scattering-in contribution is less significant for electron-atom recoil experiments, and can be minimized. Inspection of Fig. 7 shows that as the atomic detector is displaced in the $-z$ direction, less and less atoms are available to contribute to $\Delta S_a(\text{in})$. If S_a and ΔS_a are measured as a function of detector position, and an effective total cross section σ_{eff} is calculated using Eq. (1), as $\Delta S_a(\text{in})$ becomes smaller σ_{eff} will increase. This is shown in Fig. 8: for small detector displacements, σ_{eff} increases as the detector is moved away from axis, and it approaches σ asymptotically as the scattering-in contribution becomes too small to affect the measure-

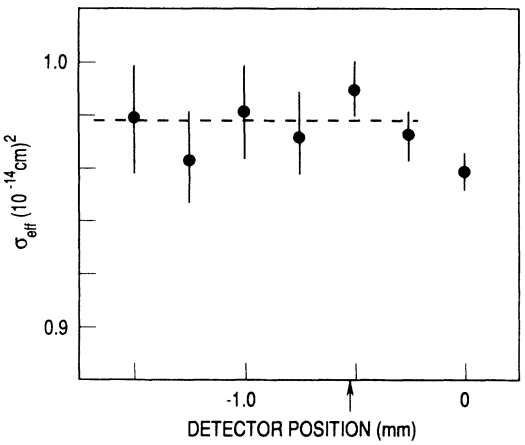

FIG. 8. Effective total collision cross sections at 12 eV vs detector position. As the detector is displaced towards the left, the scattering-in contribution to the signal is reduced, thus raising the effective cross-section value. Once the detector is displaced by 0.5 mm, the effective cross section becomes insensitive to further displacement, implying that the scattering-in contribution to the detector signal has been minimized. The arrow shows the standard detector position when accumulating data for cross-section determinations.

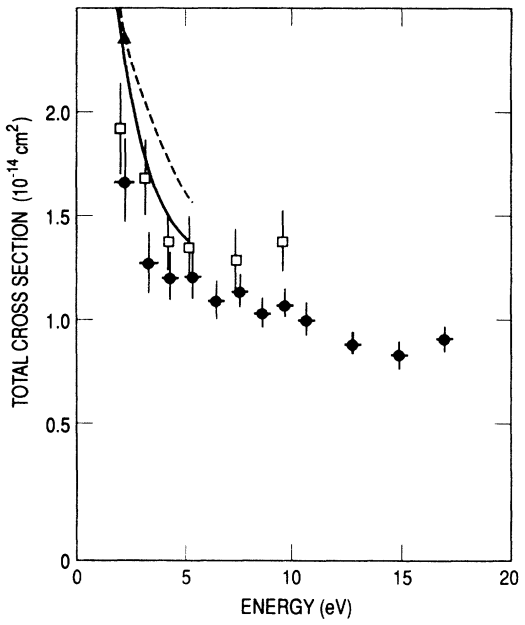

FIG. 9. Total electron–cesium-atom collision cross sections vs electron energy. Dark circles, this work; open squares, measurements by Visconti, Slevin, and Rubin (Ref. [5]); solid line, two-state close-coupling calculation by Karule and Peterkop (Ref. [19]); dashed line, two-state close-coupling calculation by Burke and Mitchell (Ref. [33]); dark triangle, five-state relativistic close-coupling calculation by Scott *et al.* (Ref. [38]). Vertical error bars indicate one standard deviation level of confidence; horizontal error bars in our data indicate the FWHM of the electron energy distribution.

ment. The cross-section measurements were made with the detector at $z = -0.55$ mm (denoted by the arrow in Fig. 8), so that the condition $\sigma_{\text{eff}} \approx \sigma$ prevailed during the experiments.

III. RESULTS

We have used the apparatus and experimental techniques described in the preceding section to measure absolute electron-cesium atom collision cross sections in the 2–18-eV impact energy range. Our results are shown by the dark circles in Fig. 9. The vertical error bars indicate one standard deviation level of confidence, and are essentially determined by the statistical errors in the measurements of S_a and $\langle 1/V \rangle$. The horizontal error bars measure the electron energy spread (FWHM). Electron energies have been corrected for contact potential differences and space-charge potential; S_a has been corrected for a small background contribution.

The VSR measurements span the 0.3–9-eV energy range; those above 2 eV are shown in Fig. 9. Also shown in Fig. 9 are the results of two-state close-coupling calculations by Karule and Peterkop [23] and by Burke and Mitchell, [37], as well as the value obtained by Scott *et al.* [38] at 2 eV in a relativistic five-state close-coupling calculation.

Comparison of our results with the VSR results shows that ours are systematically lower, although typical differences are less than a combined standard deviation. As mentioned before, the VSR results are significantly lower than those of Karule [24] (which are the lowest of the close-coupling total cross sections) below the $6P$ excitation thresholds, and agree better with those of Karule and Peterkop [23] above it. Our results would indicate that the close-coupling calculations have yielded total cross sections which are consistently high over the covered energy range.

ACKNOWLEDGMENT

This work was supported by the Aerospace Sponsored Research Program.

[1] J. Perel, P. Englander, and B. Bederson, Phys. Rev. **128**, 1148 (1962).
[2] R. E. Collins, M. Goldstein, B. Bederson, and K. Rubin, Phys. Rev. Lett. **19**, 1366 (1967).
[3] I. V. Hertel and K. J. Ross, J. Phys. B **1**, 697 (1968).
[4] W. Gehen and M. Wilmers, Z. Phys. **244**, 395 (1971).
[5] P. J. Visconti, J. A. Slevin, and K. Rubin, Phys. Rev. A **3**, 1310 (1971).
[6] D. Andrick, M. Eyb, and M. Hofman, J. Phys. B **5**, L15 (1972).
[7] M. Goldstein, A. Kasdan, and B. Bederson, Phys. Rev. A **5**, 660 (1972).
[8] D. Hils, M. V. McCusker, H. Kleinpoppen, and S. J. Smith, Phys. Rev. Lett. **29**, 398 (1972).
[9] B. Jaduszliwer, N. D. Bhaskar, and B. Bederson, Phys. Rev. A **14**, 162 (1976).
[10] J. J. McClelland, M. H. Kelley, and R. J. Celotta, Phys. Rev. Lett. **58**, 2198 (1987).
[11] F. Eschen, G. F. Hanne, K. Jost, and J. Kessler, J. Phys. B **22**, L455 (1989).
[12] X. L. Han, G. W. Schinn, and A. Gallagher, Phys. Rev. A **42**, 1245 (1990).
[13] I. V. Hertel and W. Stoll, J. Phys. B **7**, 583 (1974).
[14] S. J. Buckman and P. J. O. Teubner, J. Phys. B **12**, L583 (1979).
[15] B. Jaduszliwer, R. Dang, P. Weiss, and B. Bederson, Phys. Rev. A **21**, 808 (1980).
[16] H. W. Hermann and I. V. Hertel, Z. Phys. A **307**, 89 (1982).
[17] G. F. Hanne, Cz. Szmytkowski, and M. van der Wiel, J. Phys. B **15**, L109 (1982).
[18] B. Stumpf and A. Gallagher, Phys. Rev. A **32**, 3344 (1985).
[19] J. J. McClelland, M. H. Kelley, and R. J. Celotta, J. Phys. B **20**, L385 (1987).
[20] J. J. McClelland, M. H. Kelley, and R. J. Celotta, Phys. Rev. A **40**, 2321 (1989).
[21] M. Zuo, T. Y. Jian, L. Vuskovic, and B. Bederson, Phys. Rev. A **41**, 2489 (1990).
[22] T. S. Stein, R. D. Gomez, Y. F. Hsieh, W. E. Kauppila, C. K. Kwan, and Y. J. Wan, Phys. Rev. Lett. **55**, 488 (1985).
[23] E. M. Karule and R. K. Peterkop, in *Atomic Collisions III,* edited by V. I. Veldre (Latvian Academy of Science, Riga, 1965) (Translation JILA Information Center Report No. 3, University of Colorado, Boulder, 1966), p. 1.
[24] E. M. Karule, in *Atomic Collisions III* (Ref. 23), p. 29.
[25] L. L. Barnes, N. F. Lane, and C. C. Lin, Phys. Rev. **137**, A388 (1965).
[26] P. G. Burke and A. J. Taylor, J. Phys. B **2**, 869 (1969).
[27] D. W. Norcross, J. Phys. B **4**, 1458 (1971).
[28] D. L. Moores and D. W. Norcross, J. Phys. B **5**, 1482 (1972).
[29] H. R. J. Walters, J. Phys. B **6**, 1003 (1973).
[30] J. V. Kennedy, V. P. Myerscough, and M. R. C. McDowell, J. Phys. B **10**, 3759 (1977).
[31] J. Mitroy, E. McCarthy, and A. T. Stelbovics, J. Phys. B **20**, 4827 (1987).
[32] K. Rubin, J. Perel, and B. Bederson, Phys. Rev. **117**, 151 (1960).
[33] A. N. Nesmeyanov, *Vapor Pressure of the Chemical Elements* (Elsevier, Amsterdam, 1963), p. 445.
[34] J. R. Pierce, *Theory and Design of Electron Beams* (Van Nostrand, New York, 1954), p. 174.
[35] E. Harting and F. H. Read, *Electrostatic Lenses* (Elsevier, Amsterdam, 1976), p. 301.
[36] B. Jaduszliwer, A. Tino, P. Weiss, and B. Bederson, Phys. Rev. Lett. **51**, 1644 (1983).
[37] P. G. Burke and J. F. B. Mitchell, J. Phys. B **6**, L161 (1973).
[38] N. S. Scott, K. Bartschat, P. G. Burke, W. B. Eissner, and O. Nagy, J. Phys. B **17**, L191 (1984).